**8.9 MOLECULAR DYNAMICS MODELING OF ATOMIC DISPLACEMENT CASCADES IN 3C-SiC** – G. D. Samolyuk, Y. N. Osetskiy and R. E. Stoller (Oak Ridge National Laboratory)

## OBJECTIVE

The objective of this effort is to characterize the nature of primary radiation damage in SiC to provide a basis for understanding the experimentally observed fluence-temperature map of the irradiated microstructure. Recently reported results demonstrated that the most commonly used interatomic potentials (Tersoff [1]) are inconsistent with *ab initio* calculations of defect energetics. In order to demonstrate the sensitivity of cascade recombination to the value of barrier recombination additional cascade simulations have been done with the newly developed Gao-Weber potential [2].

## SUMMARY

We demonstrated that the most commonly used interatomic potentials are inconsistent with *ab initio* calculations of defect energetics. Both the Tersoff potential used in this work and an alternate modified embedded atom method potential reveal a barrier to recombination which is much higher than the density functional theory (DFT) results. The barrier obtained with a newer potential by Gao and Weber is closer to the DFT result but the overall energy landscape is significantly different. This difference results in a significant difference in the cascade production of points defects. We have completed both 10 keV and 50 keV pka energy cascade simulations in SiC at temperatures equal to 300, 600, 900 and 1200 K. Results were obtained for the number of stable point defects using the Tersoff/ZBL and Gao-Weber/ZBL (GW) interatomic potentials. In a contrast to Tersoff potential, the GW potential produces almost twice as many C vacancies and interstitials at the time of maximum disorder (~0.2 ps) but only about 25% more stable defects at the end of the simulation. Only about 20% of the carbon defects produced with the Tersoff potential recombine during the in-cascade annealing phase, while about 60% recombine with the GW potential. The GW potential appears to give a more realistic description of cascade dynamics in SiC, but still has some shortcomings when the defect migration barriers are compared to the *ab initio* results.

## PROGRESS AND STATUS

### Introduction

Irradiation effects in solids have received a great deal of attention since the 1960s. This attention was mostly related to metals. Designing silicon carbide components for fusion reactor blankets requires a basic understanding of defect formation and evolution, and the associated property changes. Despite the large range of phenomenological studies of observed effects, the microstructural origin of these effects is not well understood.

The molecular dynamics (MD) study of cascades evolution, based on application of empirical potential, is an important tool for understanding the irradiation effects. According to our analysis of SiC publications, most of the cascades modeling in SiC was executed with Tersoff potential. However, as we demonstrate in our research, the Tersoff potential gives unphysical large defect migration barriers. Thus, in the current investigation we investigate the number and distribution of stable point defects in cascades in SiC with both Tersoff and GW interatomic potentials.

### Simulation Method

The GW potential code was introduced in the LAMMS molecular dynamics (MD) package [3]. The good agreement between MD and first-principles calculated formation energies of twelve most typical defects were demonstrated (see Table 1).

Table 1. The formation energies (in eV) of interstitials (dumbbells $C^+$-C<100>, $C^+$-Si<100>, $Si^+$-C<100>, $Si^+$-Si<100> and tetrahedral interstitals $C_{TC}$ …), antisite defects ($C_{Si}$, $Si_C$) and vacancies (C(V), Si(V)), together with those calculated by *ab initio* methods.

| Defects | *ab initio* | Current report |
|---|---|---|
| $C^+$-C<100> | 3.16 | 3.05 |
| $C^+$-Si<100> | 3.59 | 3.44 |
| $Si^+$-C<100> | 10.05 | 7.75 |
| $Si^+$-Si<100> | 9.32 | 5.51 |
| $C_{TC}$ | 6.41 | 4.66 |
| $C_{TS}$ | 5.84 | 4.33 |
| $Si_{TC}$ | 6.17 | 3.98 |
| $Si_{TS}$ | 8.71 | 6.79 |
| $C_{Si}$ | 1.32 | 1.69 |
| $Si_C$ | 7.20 | 7.94 |
| C(V) | 5.48 | 2.77 |
| Si(V) | 6.64 | 3.30 |

To improve weak repulsive of GW potential at short distances we joined GW with well-established Ziegler, Biersack and Littmark (ZBL) potential at 0.95 Å (see Figure 1).

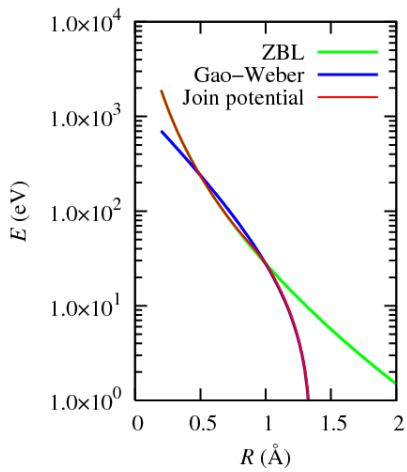


**Figure 1.** Repulsive Si-C atom interaction. The GW potential is shown in blue, the ZBL in green and the resulting joined potential is shown by the red line.

Simulation cells containing from 80x80x80 unit cells (409,600 atoms) were used for 10 keV primary knock-on atom (PKA) kinetic energy cascades and 120x120x120 unit cells (13,824,000 atoms) for 50 keV PKA cascades. The initial system was equilibrated for 2 picoseconds with time steps of 0.1 femtosecond. Each cascade was initiated by giving a Si atom the kinetic energy of 10 or 50 keV while holding zero total momentum. The cascades evolved for 20 ps and the time step is modified such that the distance traveled by the fastest particle in the system is less than 0.014 Å. Constant volume is held through the iteration and the lattice parameter is chosen for zero system pressure in equilibrium at a particular temperature. The Wigner-Seitz cell analysis method was used to determine defects in the modeling system.

The *ab initio* recombination barrier was calculated within the density functional theory (DFT) was calculated using the Quantum ESPRESSO (QE) package [4]. The calculations have been done using a plane-wave basis set and ultrasoft pseudo-potential [5] optimized in RRKJ scheme [6] (Si.pbe-n-rrkjus.UPF, C.pbe-n-rrkjus.UPF from QE pseudopotentials database). We used Perdew, Burke, and Ernzerhof [7] exchange-correlation functional. The Brillouin zone (BZ) summations were carried out over

a 4 × 4 × 4 BZ grid for the system with 64 atoms in a supercell. The electronic smearing with a width of 0.02 Ry was applied according to the Methfessel-Paxton method. The plane wave energy cut off 40 Ry and charge density - 400 Ry allows reaching accuracy 0.2 mRy/atom. Atomic structure was optimized until the forces were smaller than 0.001 Ry/Å.

**Results**

The 10 keV cascade simulations with Tersoff potential were carried out at a range of temperatures and indicated that in-cascade recombination seemed to be much lower than in metals. Simulations at 50 keV have shown the same behavior as indicated in Figure 2. Figure 2a shows the time dependence of defects obtained in a 50 keV SiC cascade at 600, and Figure 2b shows typical results for similar simulations in iron. Note that the ratio of the peak defect count to the stable defect count at t>10 ps is less than a factor of two in SiC and almost two orders of magnitude in iron.

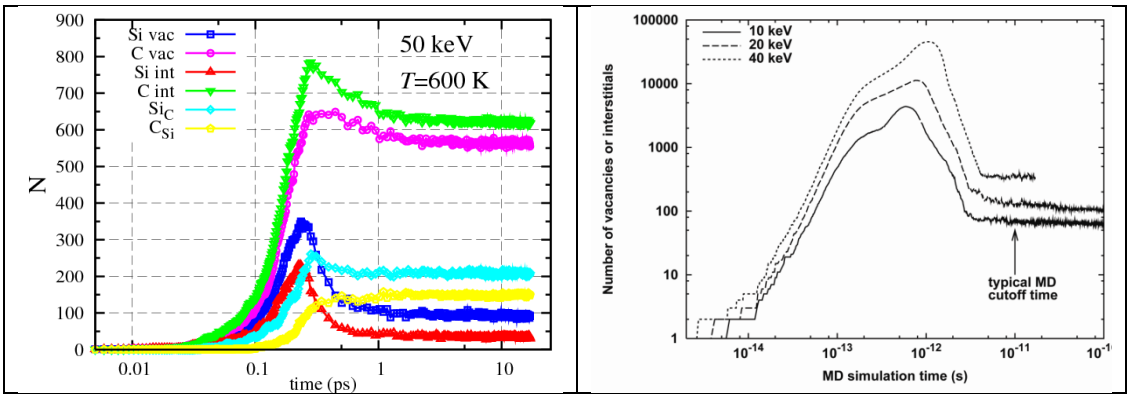


**Figure 2.** Time dependence of the number of point defects observed in MD displacement cascade simulations: (a) 50 keV SiC cascade at 600 K with Tersoff potential and (b) 10, 20, and 40 keV cascades in iron.

Such significant difference between SiC and Fe results is caused by presence of “empty” spaces in SiC lattice at (1/2, 1/2, 1/2), (3/4, 3/4, 3/4) and symmetry related positions which easily accommodate interstitial atoms.

Point defects in SiC consist of interstitials (I) and vacancies (V) of both carbon and silicon, as well as antisite defects of C on an Si site ($C_{Si}$) and Si on a C site ($Si_C$). The carbon defects predominate as shown by the green and purple symbols in Figure 3.

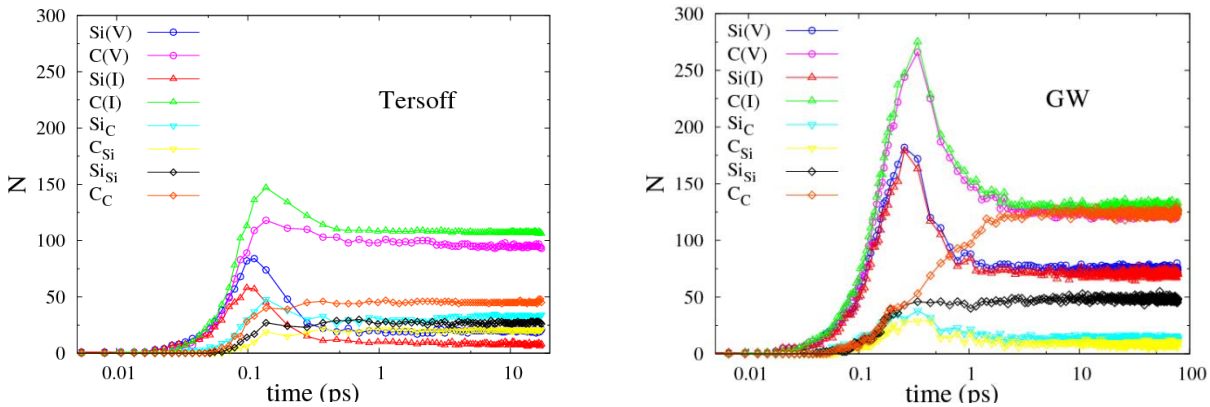


**Figure 3.** Time dependence of the number of point defects observed in MD displacement cascade simulations 10 keV pka at 300 K: (a) Tersoff potential, (b) GW potential.

This result is qualitatively similar to that obtained with Tersoff potential (Figure 3b). However, in contrast to the simulations with the Tersoff potential, the GW potential (Figure 3b) produces almost twice as many C vacancies and interstitials at the time of maximum disorder (~0.2 ps) but only about 25% more stable defects at the end of the simulation. As a result the ratio of peak-to-stable defects is much higher for the GW potential. This result is more similar to that observed in metals and oxides. Only about 20% of the carbon defects produced with the Tersoff potential recombine during the in-cascade annealing phase, while about 50% recombine with the GW potential.

As discussed in our earlier reports, the energy barrier for carbon V-I recombination with the GW potential is much smaller than with the Tersoff potential barrier, and is closer to results of first-principles calculations (Figure 4). On the basis of these result we can conclude that GW potential gives a much more realistic description of cascade dynamics in SiC and we will use this potential in our continuing work.

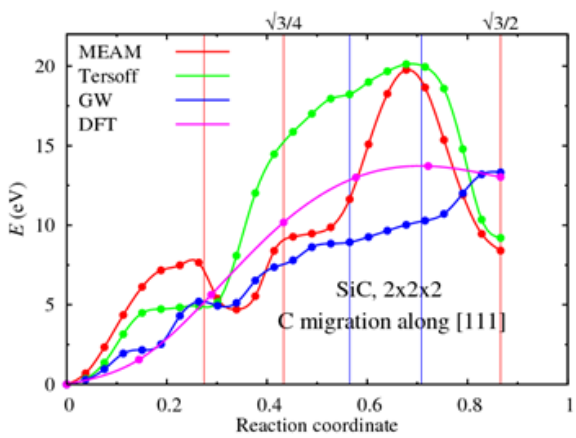


**Figure 4.** Carbon atom migration barrier in [111] direction.

The results for cluster size distributions at the end of simulation for both potentials are presented in Figure 5. In our analysis we defined group of point defects as a linked cluster if any of them are connected by a distance less than a lattice parameter. Both simulations produce a significant amount of pair clusters and ~ 75 % of these clusters correspond to the same atom type I-V pair. However if in the case of Tersoff

potential all I-V pair clusters correspond to carbon atoms, in the case of GW potential a significant part of these clusters correspond to silicon.

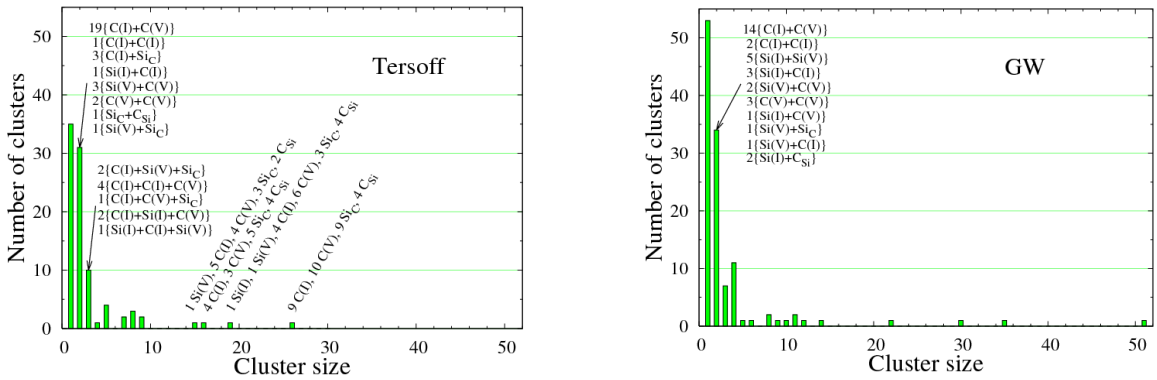


**Figure 5.** Cluster size distribution at the end of 10 keV Si recoil event in SiC at 300 K: (a) Tersoff potential, (b) GW potential.

Another difference corresponds to large size cluster distributions. Thus in the case of Tersoff potential (Figure 5a) there are only two relatively large clusters containing 19 and 21 defects, in the case of GW potential there are four clusters of size 21, 30, 35 and 51 defects. These large clusters could be discussed as potential amorphisation regions. One of these clusters containing 51 defects is presented in Figure 6, where carbon defects predominate as shown by the green and purple symbols.

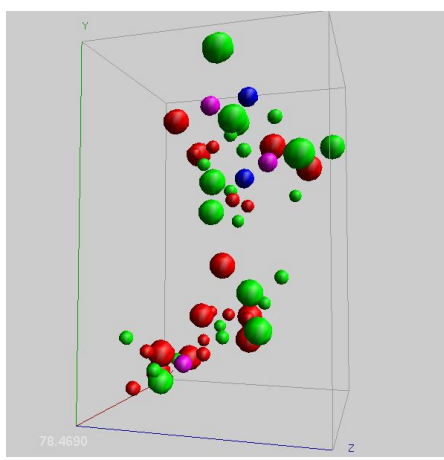

**Figure 6.** The distribution of carbon (green) and silicon (red) interstitials (large spheres) and vacancies (small spheres) at the end of 10 keV Si recoil event in SiC. Blue and purples spheres correspond to $Si_C$ and $C_{Si}$ antisites, respectively.

The number of defects at the end of cascade evolution is weakly temperature dependent for Tersoff potential, but reduces with temperature for the GW potential. The difference is due to unphysically large migration barriers for Tersoff potential. The increase in the temperature naturally leads to more rapid diffusion of carbon vacancies and interstitials. As a result, more carbon vacancies and interstitial recombine and the number of defects at the end of cascade evolution is reduced with temperature increase. However, the defect migration barriers for Tersoff potential are so large that diffusion is suppressed even at high temperatures such as 1600 K and the number of defects is weakly temperature dependent.

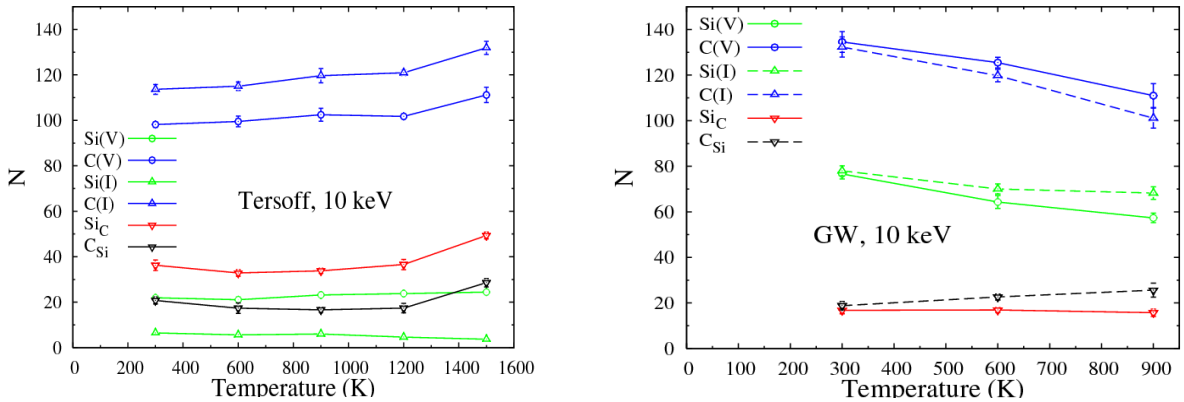


**Figure 7.** The number of defects at the end of cascade evolution

Additional computational resources have been used for this work through collaboration with JAEA.

## REFERENCES

[1] J. Tersoff, Phys. Rev. B 39 (1989) 5566–5568.
[2] F. Gao and W. J. Weber, Nucl. Instr. And Methods in Phys. Research B 191 (2002) 504-508.
[3] S. Plimpton, Fast Parallel Algorithms for Short-Range Molecular Dynamics, J Comp Phys, 117, (1995), 1-19.
[4] P. Giannozzi, S. Baroni, and N. Bonini ... Quantum espresso: a modular and open-source software project for quantum simulations of materials. J of Physics:Condensed Matter, 21, 395502 (2009).
[5] D. Vanderbilt. Soft self-consistent pseudopotentials in a generalized eigenvalue formalism. Phys. Rev. B, 41, (1990), 7892–7895.
[6] A. M. Rappe, K. M. Rabe, E. Kaxiras, and J. D. Joannopoulos. Optimized pseudopotentials. Phys. Rev. B, 41, (1990), 1227–1230.
[7] J. P. Perdew, K. Burke, and M. Ernzerhof. Generalized gradient approximation made simple. Phys. Rev. Lett., 77, (1996), 3865–3868.